U1406(H3)-ring II(6), U1406(H6)-ring IV(4‴), C1407(H4)-ring II(6), ring III(2″), C1407(H5)-ring IV(1‴, 2‴), A1408(H6)-ring I(1′) ring II(6), G1489(H8)-ring IV(4‴), U1490(H5)-ring III(3″, 4″, 5″) ring IV(3‴, 4‴, 5‴, 6‴), U1490(H6)-ring II(5″), G1491(H1)-ring I(1′), G1491(H2′)-ring I(3′, 4′), G1491(H3′)-ring I(2′, 3′), A1492(H3′)-ring I(3′, 4′, 5′), A1492(H5′)-ring I(3′), A1493(H2′)-ring II(3), A1493(H3′-ring II(2 equatorial, 3), A1493(H5′)-ring II(3), A1493(H8)-ring I(3′, 4′, 5′) ring II(2 axial), G1494(H1)-ring II(2 axial, 2 equatorial, 6), G1494(H3′)-ring II(2 axial, 2 equatorial), U1495(H5)-ring II(1, 2 axial, 2 equatorial, 3, 6), U1495(H3)-ring II(6).

14. RNA dihedral restraints were assigned following the general strategy of Varani and co-workers [F. H.-T. Allain and G. Varani, *J. Mol. Biol.* **250**, 333 (1995)]. β-Dihedral angles were restrained from estimates of the $^3J_{P\text{-}H5'}$, $^3J_{P\text{-}H5''}$, and $^3J_{P\text{-}C4'}$ coupling constants from the HP-COSY and HCP experiments [J. P. Marino *et al.*, *J. Am. Chem. Soc.* **116**, 6472 (1994)]. When evidence for a trans β angle was observed, this angle was restrained to 180 ± 30°. ε was restrained from estimates of $^3J_{H3'\text{-}P}$, $^3J_{C2'\text{-}P}$, and $^3J_{C4'\text{-}P}$ from HP-COSY and HCP. Constraints of 210 ± 30° (trans) or 260 ± 30° (gauche$^-$) or 235 ± 55° (when the trans or gauche$^-$ conformations could not be distinguished) were used. The γ dihedral angles were constrained from estimates of $^3J_{H4'\text{-}H5'}$ and $^3J_{H4'\text{-}H5''}$ coupling constants from the ^{31}P decoupled DQF-COSY and the 3D HMQC-TOCSY experiment with a short (20 ms) mixing time. For a gauche$^+$ conformation, γ was constrained to 55 ± 30° (or ±40°). The ribose sugar pucker was estimated from analysis of $^3J_{H1'\text{-}H2'}$ in the ^{31}P decoupled DQF-COSY spectrum. Ribose conformation was restrained to $C_{2'}$-*endo* (δ = 160 ± 30°) or $C_{3'}$-*endo* (δ = 85 ± 30°) when $^3J_{H1'\text{-}H2'}$ was >8 Hz or <3 Hz, respectively. No restraints were used for riboses with mixed sugar conformations. Several paromomycin ring I and II dihedral angles were restrained from analysis of the short mixing time TOCSY and DQF-COSY spectrum.
15. Structures were calculated using a simulated annealing protocol within the InsightII NMRArchitect package (Biosym Technologies, San Diego, CA). A randomized array of atoms corresponding to RNA and paromomycin was heated to 1000 K, and bonding, distance and dihedral restraints, and a repulsive quartic potential were gradually increased to full value over 40 ps of molecular dynamics. The molecules were then cooled during 10 ps to 300 K and subjected to a final energy minimization step that included an attractive Lennard-Jones potential. No electrostatic term was included in the target function. Using this protocol, 30% of the structures converged, as based on restraint violation energies, and 30 of them were collected to be further refined with the final set of restraints. There were differences of greater than 100 kcal · mol^{-1} between converged and unconverged structures. During refinement, molecules were heated to 1000 K and subject to 30 ps of molecular dynamics following the same protocol as above. The molecules were then cooled during 10 ps to 300 K and subjected to a final energy minimization step that again included an attractive Lennard-Jones potential and no electrostatic term. A total of 392 distance restraints were used including 91 intranucleotide RNA restraints, 198 internucleotide RNA, 43 base pair hydrogen bonding restraints, 13 interesidue paromomycin restraints, and 47 RNA-paromomycin restraints; no hydrogen bonding restraints were used for non-canonical base pairs. A total of 154 experimental dihedral restraints were used, comprising 8 paromomycin and 146 RNA restraints. Additional restraints were used to maintain chirality, and base pair planarity outside the internal loop of the RNA. The final force constants for distance restraints were 40 kcal · mol^{-1}. Base pairing hydrogen bond and dihedral restraints final force constants were set to 60 kcal · mol^{-1}. All color figures were generated with the program InsightII (Biosym Technologies, San Diego, CA).
16. K. J. Baeyens, H. L. De Bondt, S. R. Holbrook, *Nature Struct. Biol.* **2**, 56 (1995).
17. The A1408-A1493 pair geometry was defined by distance restraints derived from ^{15}N-correlated NOESY experiments for exchange-broadened protons [L. Mueller, P. Legault, A. Pardi, *J. Am. Chem. Soc.* **117**, 11043 (1995)] performed on the complex containing specifically ^{15}N-, ^{13}C-labeled adenines. Adenine amino nitrogens were assigned by through-bond correlation to H8 and H2 protons after 2D and 3D HNC-TOCSY-CH experiments [J. P. Simorre, G. R. Zimmermann, L. Mueller, A. Pardi, *J. Am. Chem. Soc.* **118**, 5316 (1996)]. The ε angle for A1493 adopts a *gauche*$^-$ conformation, and the torsion angle α for the phosphate between G1491 and A1492 adopts a trans conformation. The latter is consistent with the downfield chemical shift of the corresponding ^{31}P resonance, even though this information was not used during calculations.
18. D. G. Reid and K. Gajjar, *J. Biol. Chem.* **262**, 7967 (1987).
19. S. Blanchard and J. D. Puglisi, unpublished results.
20. R. Benveniste and J. Davies, *Antimicrob. Agents Chemother.* **4**, 402 (1973).
21. G. Dirheimer, G. Keith, P. Dumas, E. Westhof, in *tRNA Structure, Biosynthesis, and Function*, D. Söll and U. L. RajBhandary, Eds. (American Society for Microbiology, Washington, DC, 1995), pp. 93–126.
22. J. M. Wilhelm, S. E. Pettitt, J. J. Jessop, *Biochemistry* **17**, 1143 (1978).
23. E. A. DeStasio, D. Moazed, H. Noller, A. E. Dahlberg, *EMBO J.* **8**, 1213 (1989); E. A. DeStasio and A. E. Dahlberg, *J. Mol. Biol.* **212**, 127 (1990).
24. S. Yoshizawa and J. D. Puglisi, unpublished results.
25. H. J. Grosjean, S. De Henau, D. M. Crothers, *Proc. Natl. Acad. Sci. U.S.A.* **75**, 610 (1978).
26. J. J. Hopfield, *ibid.* **71**, 4135 (1974); J. Ninio, *Biochimie* **57**, 587 (1975).
27. A. P. Patapov, F. J. Triana-alonso, K. Nierhaus, *J. Biol. Chem.* **270**, 17680 (1995).
28. A. M. Pyle and T. R. Cech, *Nature* **350**, 628 (1991); A. M. Pyle, F. L. Murphy, T. R. Cech, *ibid.* **358**, 123 (1992).
29. M. V. Rodnina, T. Pape, R. Fricke, L. Kuhn, W. Wintermeyer, *J. Biol. Chem.* **271**, 646 (1996).
30. We thank H. Noller for encouragement and discussions, A. Pardi for assistance with NMR techniques, E. V. Puglisi for comments and support, and M. Ares and R. Green for reading the manuscript. Supported by grants from the Packard Foundation, the Deafness Research Foundation, National Institute of Health (GM51266-01A1), Lucille P. Markey Charitable Trust (J.D.P.), and a postdoctoral grant from Institut National de la Santé et de la Recherche Médicale (D.F.). The coordinates have been deposited in the Brookhaven Protein Data Bank with access number T9496.

26 April 1996; accepted 13 September 1996

Major Susceptibility Locus for Prostate Cancer on Chromosome 1 Suggested by a Genome-Wide Search

Jeffrey R. Smith,* Diha Freije,* John D. Carpten,* Henrik Grönberg,* Jianfeng Xu,* Sarah D. Isaacs, Michael J. Brownstein, G. Steven Bova, Hong Guo, Piroska Bujnovszky, Deborah R. Nusskern, Jan-Erik Damber, Anders Bergh, Monika Emanuelsson, Olli P. Kallioniemi, Jennifer Walker-Daniels, Joan E. Bailey-Wilson, Terri H. Beaty, Deborah A. Meyers, Patrick C. Walsh, Francis S. Collins, Jeffrey M. Trent,† William B. Isaacs

Despite its high prevalence, very little is known regarding genetic predisposition to prostate cancer. A genome-wide scan performed in 66 high-risk prostate cancer families has provided evidence of linkage to the long arm of chromosome 1 (1q24-25). Analysis of an additional set of 25 North American and Swedish families with markers in this region resulted in significant evidence of linkage in the combined set of 91 families. The data provide strong evidence of a major prostate cancer susceptibility locus on chromosome 1.

Prostate cancer is the most common malignancy diagnosed in U.S. males, accounting for more than 40,000 deaths in this country annually (*1*). African Americans have the highest incidence and mortality rates of any population studied (*2*). Numerous studies have provided evidence for familial clustering of prostate cancer, indicating that family history is a major risk factor for this disease (*3–5*). Segregation analysis of familial prostate cancer suggests the existence of at least one dominant susceptibility locus and predicts that rare high-risk alleles at such loci account in the aggregate for 9% of all prostate cancers and more than 40% of early onset disease (*6*).

Analyses of genetic alterations in prostate cancer have demonstrated frequent duplication of DNA sequences on the distal long arm of chromosome 8 (*7*), as well as loss of DNA sequences resulting in loss of heterozygosity (LOH) for the short arm of chromosome 8 and the long arm of chromosome 13 (*8, 9*). Preliminary investigations by linkage analysis of these regions as well as sites of known tumor suppressor genes have not identified a susceptibility locus in prostate cancer (*10, 11*).

Prostate cancer presents a number of serious obstacles to linkage analysis. The prevalence is extremely high; there is a one in five lifetime probability of prostate cancer diagnosis in U.S. males (*1*). This potentially could

result in a high rate of phenocopies; individuals whose prostate cancers result from very different causes. The late age of onset [less than 0.1% of prostate cancer cases are diagnosed under the age of 40 (*1*)] leads to general lack of available samples from an affected individual's ancestors. These obstacles are complicated by the absence of known clinical features (other than age of onset) that might allow subgrouping of prostate cancer families to reflect potential genetic heterogeneity (5). Finally, it is difficult to find extended pedigrees that are highly informative for linkage (in other words, that contain large numbers of affected family members) (*12*).

In spite of these difficulties, we have undertaken a linkage analysis to search for evidence of loci contributing to risk for prostate cancer in a group of 79 North American and 12 Swedish pedigrees, each having at least three first-degree relatives affected with prostate cancer. These families were selected on the basis of the number of affected males from which samples could be obtained for typing, either as blood samples or archival specimens and the absence of evidence of bilineal inheritance (*13*). A summary of the characteristics of the families studied is given in Table 1. Overall, affected individuals in these families had an average age of diagnosis of 65, with a total of 34 males diagnosed before the age of 55.

To search for the location of high-risk alleles for prostate cancer, a genome-wide scan was performed in a subgroup of 66 North American families. A total of 341 dinucleotide repeat markers were analyzed in these pedigrees to complete a map with a marker density of 10 cM (*14*), requiring more than 130,000 genotypes. On average, 79% of our study group were heterozygous for each marker. For the parametric analysis of the genotype data, we used a model of dominant inheritance that includes a fixed phenocopy rate of 15% and the assumption that unaffected men over the age of 75 are not likely to be gene carriers (*15*). A plot of two-point lod (logarithm of the likelihood ratio for linkage) scores (*16*) for the genome-wide scan ($\hat{Z}$) is shown in Fig. 1. The highest lod score observed was 2.75 with marker *D1S218*, which maps to the distal long arm of chromosome 1 (1q24-25). As chromosome 1 showed the most significant evidence for linkage, additional markers in this region were typed in the original 66 families as well as in an additional group of 25 families, 12 of which were collected in Sweden (*13*). These analyses provided additional evidence for linkage in the 1q24-25 region with a maximum two-point lod of 3.65 at recombination fraction $\Theta = 0.18$ with marker *D1S2883* (Table 2).

As parametric analyses are model-dependent, we also used nonparametric analyses to further examine linkage data in this region (*16*). Nonparametric multipoint linkage (NPL) Z scores are given for this analysis in Table 2. Highly significant *P*-values were obtained for multiple markers, providing further evidence for linkage in this region. To determine the most likely location for the susceptibility locus, parametric multipoint analyses were performed with various combinations of markers in this region. Lod scores >4 were obtained, but did not allow unequivocal placement of the susceptibility locus due to apparent genetic heterogeneity. Significant evidence for locus heterogeneity ($\chi^2 = 8.11$, $P = 0.004$) (*16*) was obtained by an admixture test with an estimate of 34% of the families being linked to the region. The maximum multipoint lod score with markers *D1S2883*, *D1S158*, and *D1S422* under the assumption of heterogeneity was 5.43, with the postulated susceptibility locus mapping close to *D1S422* (Fig. 2). No clinical features appeared to distinguish families showing linkage to chromosome 1 from the nonlinked pedigrees.

The risk of prostate cancer in siblings of affected individuals is modified by the age of diagnosis (6). Subgrouping families by age of diagnosis, either by mean age within a family or by number of men diagnosed under age 55, provided little evidence that the families showing linkage to chromosome 1 had an earlier onset of prostate cancer than the unlinked families. However, because of difficulties in equating age of diagnosis with age of onset (*17*), further analysis will be necessary to support this conclusion.

Both African-American families analyzed in this study showed linkage to this region, yielding a combined lod score of 1.4. As there is evidence of linkage in Caucasian families in Sweden and North America as well, alterations in the 1q24-25 region may increase prostate cancer susceptibility in a variety of populations and ethnic backgrounds.

LOH studies have not previously implicated the chromosomal region 1q24-25 in

Table 1. Prostate cancer families.

Sample	Number of families	Average number per family (range)		Average age of diagnosis (range)
		Affected	Typed*	
North American	79	5.1 (3–15)	3.7 (2–11)	64.3 (39–85)
Swedish	12	3.9 (3–5)	3.6 (3–5)	69.3 (56–76)
Total	91	4.9 (3–15)	3.7 (2–11)	64.9 (39–85)

*Typed refers to the number of affected family members analyzed.

J. R. Smith, J. D. Carpten, O. P. Kallioniemi, J. Walker-Daniels, J. E. Bailey-Wilson, F. S. Collins, J. M. Trent, National Center for Human Genome Research, National Institutes of Health, Bethesda, MD.
D. Freije, H. Grönberg, S. D. Isaacs, G. S. Bova, H. Guo, P. Bujnovszky, D. R. Nusskern, P. C. Walsh, W. B. Isaacs, James Buchanan Brady Urologic Institute; J. Xu and D. A. Meyers, Department of Medicine, Johns Hopkins University, School of Medicine, Baltimore, MD.
M. J. Brownstein, National Institute of Mental Health, National Institutes of Health, Bethesda, MD.
T. H. Beaty, Department of Epidemiology, Johns Hopkins University, School of Hygiene and Public Health, Baltimore, MD.
J. R. Smith, Department of Internal Medicine, University of Michigan, Ann Arbor, MI.
H. Grönberg and M. Emanuelsson, Department of Oncology; J.-E. Damber, Department of Urology; A. Bergh, Department of Pathology, Umeå University, Umeå, Sweden.

*These authors contributed equally to this study.
†To whom correspondence should be addressed. E-mail: jtrent@nchgr.nih.gov

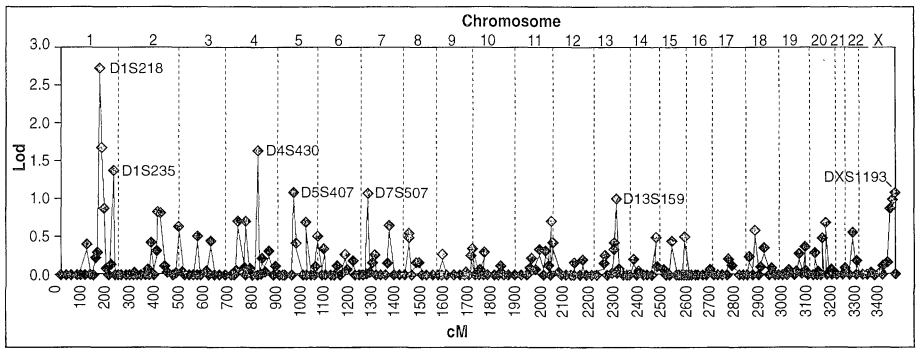

Fig. 1. Two-point lod scores for the genome-wide scan. Affected and unaffected individuals in 66 prostate cancer pedigrees were genotyped at 341 loci throughout the genome. Maximum two-point lod scores were calculated and the results plotted as a function of marker location in centimorgans. Chromosomal number is designated at the top of the plot.

prostate cancer, although analysis of cancer DNA from hereditary cases is lacking. A study by Cher *et al.* (*8*) did indicate that a large portion of the q arm including the 1q24-25 region is frequently increased in copy number in advanced prostate cancer specimens examined by comparative genomic hybridization. Candidate genes in the interval implicated include the *ski*, *abl2*, and *trk* oncogenes as well as *LAMC2*, which encodes an isoform subunit of a basement membrane protein (laminin) (*18*).

The data presented here indicate that a susceptibility locus that may account for a significant fraction of hereditary prostate cancer can be detected in families by linkage analysis. If this linkage is confirmed in an independent data set, then we propose the designation *HPC1* (hereditary prostate cancer 1) for this locus. This observation if confirmed sets the stage for the challenging task of cloning *HPC1* and identifying the responsible genetic alterations in high-risk families. Given that previous segregation analyses have suggested that approximately one in 170 individuals in the United States may carry a dominant susceptibility allele for prostate cancer (*6*), one can estimate (very roughly) that one in 500 may have an alteration in *HPC1*. Because early diagnosis can be lifesaving in prostate cancer, the potential ability to identify individuals at genetically high risk, especially when combined with methods that detect early signs of malignancy (physical exam, transrectal ultrasound, and prostate-specific antigen), could ultimately be of significant medical benefit.

Table 2. Linkage results for susceptibility to prostate cancer and nine markers on chromosome 1 in 91 families. $\hat{Z}$ and $\hat{\Theta}$ represent the maximum lod scores and recombination fractions, respectively. NPL *Z* scores are not directly comparable to parametric $\hat{Z}$ (LOD) scores. Therefore, significance levels are given for the NPL *Z* scores. For parameter (LOD) scores, a *Z* score of 3.0 corresponds to a signifiance level of a 0.0001.

Marker	Distance (cM)*	Parametric analysis: two-point lod		Nonparametric multipoint analysis	
		$\hat{Z}$	$\hat{\Theta}$	*Z* score	*P*
D1S452	—	0.94	0.27	2.28	0.01
D1S218†	1.9	2.31	0.23	2.14	0.02
D1S212	3.6	2.98	0.19	4.22	0.00001
D1S2883	0.0	3.65	0.18	4.16	0.00002
D1S466	5.1	2.41	0.20	4.71	0.000001
D1S2818	0.9	1.69	0.24	4.66	0.000002
D1S158	1.5	2.53	0.21	4.62	0.000002
D1S422	4.4	2.67	0.20	4.26	0.00001
D1S413†	4.9	1.80	0.21	2.83	0.002

*Distances in centimorgans from the preceding marker in the table were derived from the CRIMAP analysis. †Markers used in genome-wide scan.

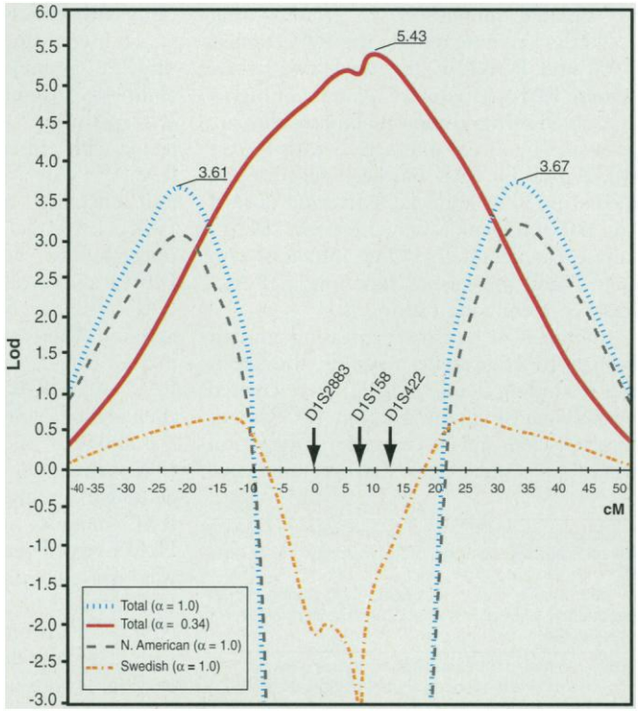

Fig. 2. Multipoint lod scores for the prostate cancer susceptibility locus relative to markers in the 1q24-25 region. Parametric multipoint lod scores were calculated with markers *D1S2883*, *D1S518*, and *D1S422*. The results are plotted as a function of distance from *D1S2883*, and are given for the North American and Swedish families, calculated both independently and combined. The combined values (total) are plotted for values of $\alpha = 1.0$ (assuming all families linked) and for $\alpha = 0.34$ (assuming heterogeneity, with 34% of the families linked). The maximum lod score under homogeneity is 3.67, but it rises to 5.43 if heterogeneity is assumed.

REFERENCES AND NOTES

1. S. L. Parker, T. Tong, S. Bolden, P. A. Wingo, *CA. Cancer J. Clin.* **46**, 5 (1996).
2. O. W. Brawley and B. S. Kramer, in *Comprehensive Textbook of Genitourinary Oncology*, N. J. Vogelsang, P. T. Scardino, W. U. Shipley, D. S. Coffey, Eds. (Williams and Wilkins, Baltimore, 1996), p. 565.
3. L. Cannon *et al.*, *Cancer Surveys* **1**, 47 (1982).
4. G. D. Steinberg, B. S. Carter, T. H. Beaty, B. Childs, P. C. Walsh, *Prostate* **17**, 337 (1990).
5. B. S. Carter *et al.*, *J. Urol.* **150**, 797 (1993).
6. B. S. Carter, T. H. Beaty, G. D. Steinberg, B. Childs, P. C. Walsh, *Proc. Natl. Acad. Sci. U.S.A.* **89**, 3367 (1992).
7. T. Visakorpi *et al.*, *Cancer Res.* **55**, 342 (1995); C. Van Den Berg *et al.*, *Clinical Cancer Res.* **1**, 11 (1995).
8. M. L. Cher *et al.*, *Cancer Res.* **56**, 3091 (1996).
9. W. B. Isaacs, in *Genetics and Cancer: A Second Look*, B. A. Ponder, W. K. Cavenee, E. Solomon, Eds. (Cold Spring Harbor Laboratory Press, Plainview, NY, 1995), p. 357.
10. L. A. Cannon-Albright *et al.*, *Am. J. Hum. Genet.* **55**, A147 (1994).
11. D. Freije *et al.*, *Proc. Am. Assoc. Cancer Res.* **37**, 670 (1996).
12. In response to an article in *Parade* magazine (3 March 1996) describing this study, individuals in 1904 different families reported having three or more family members affected with prostate cancer. Of these, 6% reported having five affected family members, 1.4% reported having six affected members, and 1.4% reported having seven or more affected members.
13. North American prostate cancer families were obtained from three sources: 65% of the families were identified by referrals generated as a response to a letter sent by one of us (PCW) to 8000 urologists throughout the country; the second source, accounting for 23% of the families, was identified by family history records of the patient population seen at Johns Hopkins Hospital for treatment of prostate cancer; the remainder of the families responded to articles published in a variety of lay publications describing this study. Prostate cancer diagnosis was verified by medical records for each affected male studied. Swedish families were obtained as a result of a nationwide search of cancer registries, and from referrals from urologists. All individuals in this study gave full informed consent.
14. Genomic DNA was prepared from lymphoblastoid transformed cell lines for the original 66 families, and prepared from whole blood and archived tissue specimens for the additional cohort of 25 families. Overall, samples from 604 individuals were genotyped (339 affected and 265 unaffected individuals); 70 additional unrelated individuals (20 North American and 50 Swedish) were also typed to provide allele frequency estimates for these populations (see *16*). High-throughput, semi-automated genotyping was accomplished by means of ABI 373 and 377 DNA sequencers to resolve multiple, fluorescently labeled markers in each gel lane. An internal size standard enabled allele sizing with the local Southern algorithm in GENESCAN (Applied Biosystems, Foster City, CA). A control individual was typed on each gel as a sizing and binning check. Genotype editing and binning were performed in GENOTYPER (Applied Biosystems, Foster City, CA). All genotyping was done blinded to affected status. A total of 26% of the markers applied were proprietary to the ABI PRISM mapping set; the balance were derived from the Genome Database (Johns Hopkins University School of Medicine, Baltimore, MD). A list of survey markers used will be supplied by the authors upon request. Reverse primer sequences for most markers were modified to promote complete nontem-

plated nucleotide addition to the 3′ end of amplified products by Taq DNA polymerase, enabling reliable identification of 1–base pair alleles present in 7.4% of the markers [M. J. Brownstein, J. D. Carpten, J. R. Smith, *Biotechniques* **20**, 1004 (1996)]. We obtained 97.1% of data sought with survey markers. Blinded duplicate typing of 7560 alleles provided a genotyping error rate estimate of 0.26%. The observed rate of non-Mendelian inheritance was 7.06×10^{-4}.

15. In the model used, affected men were assumed to be carriers of a rare autosomal dominant gene frequency $q = 0.003$) (*6*), with a fixed 15% phenocopy rate, while all unaffected men under 75 and all women were assumed to be of unknown phenotype. In men over age 75, the lifetime penetrance of gene-carriers was estimated to be 63% (based on a population based segregation analysis performed by H.G., in preparation, and the lifetime risk of prostate cancer for non-carriers was 16% in this age class (based on SEER data) [C. L. Kosary, L. A. G. Ries, B. A. Miller, B. F. Hankey, A. Harras, B. K. Edwards (Eds.), SEER Cancer Statistics Review, 1973–1992: Tables and Graphs, National Cancer Institute. NIH Pub. No. 96-2789. Bethesda, MD, 1995]. This is a conservative model as it minimizes the chances of incorrectly assuming that a young unaffected male is a noncarrier. The fact that nonparametric methods produce results of similar statistical significance (Table 2) adds confidence to the conclusion that the observed linkage is not strongly dependent on the choice of this particular model.
16. Standard parametric likelihood analysis was performed by means of FASTLINK [R. W. Cottingham Jr., R. M. Idury, A. A. Schaffer, *Am. J. Hum. Genet.* **53**, 252 (1993)] for two-point linkage and VITESSE [J. R. O'Connel and D. E. Weeks, *Nature Genet.* **11**, 402 (1995)] for multipoint linkage analysis. Multipoint analysis has the advantage of utilizing data from multiple linked markers to maximize the information in a given pedigree. Nonparametric multipoint analysis, which is robust even when the mode of inheritance is not known, was also performed, with GENEHUNTER [L. Kruglayk and E. S. Lander, *Am. J. Hum. Genet.* **57**, 439 (1995)] to calculate normalized Z scores and associated P values. In all of the linkage analyses, allele frequencies for the markers were estimated from independent individuals in the families and unrelated individuals separately for the North American and Swedish families. CRIMAP [E. S. Lander and P. Green, *Proc. Natl. Acad. Sci. U.S.A.* **84**, 2363 (1987)] was used to order the multiple markers on chromosome 1 using the genotype data from all pedigrees. The BUILD option of CRIMAP was first used to establish the order of markers with at least a likelihood ratio of 1000:1. The FLIP option was then used to calculate the likelihood of alternative marker orders by permuting adjacent loci (five flanking markers). The most likely order thus determined is the same as the published order (http://cedar.soton.ac. uk/pub). The admixture test as implemented in HOMOG [J. Ott, *Analysis of Human Genetic Linkage* (Johns Hopkins Univ. Press, Baltimore, 1985), pp. 200–203] was used to test for genetic heterogeneity in the context of the two-point parametric analysis.
17. The evaluation of age as a variable is confounded because of the changing methods used to diagnose this disease, and increased interest in screening for this disease. For the years prior to the use of prostate-specific antigen (PSA), diagnosis of prostate cancer was often not made until men presented with advanced disease, whereas today most men are diagnosed younger and at an earlier stage.
18. The expert technical assistance of C. Ewing and J. Robinson, and the help of X. Chen, D. Schwengel, R. Paul, C. Engstrand, A. Kallioniemi, L. Hardie, and B. Carter during the early phases of this work is acknowledged. We also thank B. Childs, J. Isaacs, and D. Coffey for helpful advice. We acknowledge the assistance of L. Middelton, C. Francomano, and the Family Studies Core of the National Center for Human Genome Research (NCHGR), and the Genetic Resources Core Facility (JHU). We also acknowledge A. Lowe and D. Gilbert at the Applied Biosystems Division of Perkin-Elmer for providing valuable genotyping technical support. We wish to thank all the physicians who referred families for this study. Supported by grants from U.S. Public Health Service SPORE CA58236; The Fund for Research and Progress in Urology; The Johns Hopkins University; Swedish Cancer Society (Cancerfonden); Lion's Cancer Foundation, Department of Oncology, Umeå Universitet, and a 1995 CaPCURE award. D.F. is supported by a grant from American Foundation for Urologic Disease.

1 October 1996; accepted 24 October 1996

RAC Regulation of Actin Polymerization and Proliferation by a Pathway Distinct from Jun Kinase

Tom Joneson,* Michele McDonough,* Dafna Bar-Sagi, Linda Van Aelst†

The RAC guanine nucleotide binding proteins regulate multiple biological activities, including actin polymerization, activation of the Jun kinase (JNK) cascade, and cell proliferation. RAC effector loop mutants were identified that separate the ability of RAC to interact with different downstream effectors. One mutant of activated human RAC protein, RAC^{V12H40} (with valine and histidine substituted at position 12 and 40, respectively), was defective in binding to PAK3, a Ste20-related p21-activated kinase (PAK), but bound to POR1, a RAC-binding protein. This mutant failed to stimulate PAK and JNK activity but still induced membrane ruffling and mediated transformation. A second mutant, RAC^{V12L37} (with leucine substituted at position 37), which bound PAK but not POR1, induced JNK activation but was defective in inducing membrane ruffling and transformation. These results indicate that the effects of RAC on the JNK cascade and on actin polymerization and cell proliferation are mediated by distinct effector pathways that diverge at the level of RAC itself.

The RAC proteins have been implicated in the regulation of various fundamental cellular processes including actin cytoskeletal organization (*1*), transcriptional activation (*2*), and cell proliferation (*3–5*). To identify the effector pathways that mediate the biological activities induced by RAC, we isolated mutant RAC proteins that could discriminate among the RAC targets PAK and POR1 in the yeast two-hybrid system. PAK proteins are a family of highly conserved serine-threonine kinases that are activated by direct interaction with RAC1 (*6*). A role for PAK has been suggested in mediating RAC-induced activation of JNK and p38 mitogen-activated protein (MAP) kinase cascades (*7*). POR1 interacts with RAC1 and appears to function in RAC-induced membrane ruffling (*8*).

Libraries of vectors expressing mutant human RAC proteins fused to the LexA DNA binding domain (LBD) were created by polymerase chain reaction (PCR) mutagenesis (*9*) and screened for interaction with PAK3 and POR1. Two mutants containing a single amino acid substitution in the RAC effector loop were identified. One mutant, RAC^{V12H40}, failed to bind PAK3 but did bind POR1, and another mutant, RAC^{V12L37}, bound PAK3 but not POR1 (Table 1). Identical binding profiles were obtained for the interaction of these mutants with PAK1 (*10*).

To investigate the biological activities of the RAC mutants, we first examined their abilities to stimulate PAK and activate the JNK pathway. COS-1 cells were cotransfected with either RAC^{V12}, RAC^{V12H40}, or RAC^{V12L37} expression plasmids and a plasmid encoding a Myc-tagged version of PAK1. PAK1 activity was assayed in immunoprecipitates with myelin basic protein (MBP) as the substrate (*11*). Expression of RAC^{V12L37} resulted in stimulation of PAK activity, whereas expression of RAC^{V12H40} did not (Fig. 1, top). Thus, the activation of PAK by the RAC mutants is dependent on their ability to interact with PAK. To test for the ability of the RAC mutants to induce JNK activation, we cotransfected COS-1 cells with expression plasmids encoding RAC mutants and a plasmid encoding a FLAG-tagged version of JNK1. JNK activity was assayed with glutathione-S-transferase (GST) fused to c-Jun as the substrate (*12*). RAC^{V12H40}, which did not bind to or activate PAK, also did not stimulate JNK activity (Fig. 1, bottom). The RAC^{V12L37} mutant,

T. Joneson and D. Bar-Sagi, Department of Molecular Genetics and Microbiology, State University of New York, Stony Brook, NY 11794, USA.
M. McDonough and L. Van Aelst, Cold Spring Harbor Laboratory, 1 Bungtown Road, Cold Spring Harbor, NY 11724, USA.

*These authors contributed equally to this work.
†To whom correspondence should be addressed.